Imaging the Energy Deposited by a 20 MeV Proton Beam Using a Commercial Liquid Scintillator

Peter Hobson[1], Maria Maxouti[2], Jeffrey Bamber[3], Kenneth Long[2]

[1]Queen Mary University of London, [2]Imperial College London, [3]Institute of Cancer Research and Royal Marsden NHS Foundation Trust

Last revised 7 July2024

Ion Therapy Research Facility

Vision:

Transform clinical practice of proton/ion-beam therapy by creating a fully automated, highly flexible system to harness the unique properties of laser-driven ion beams

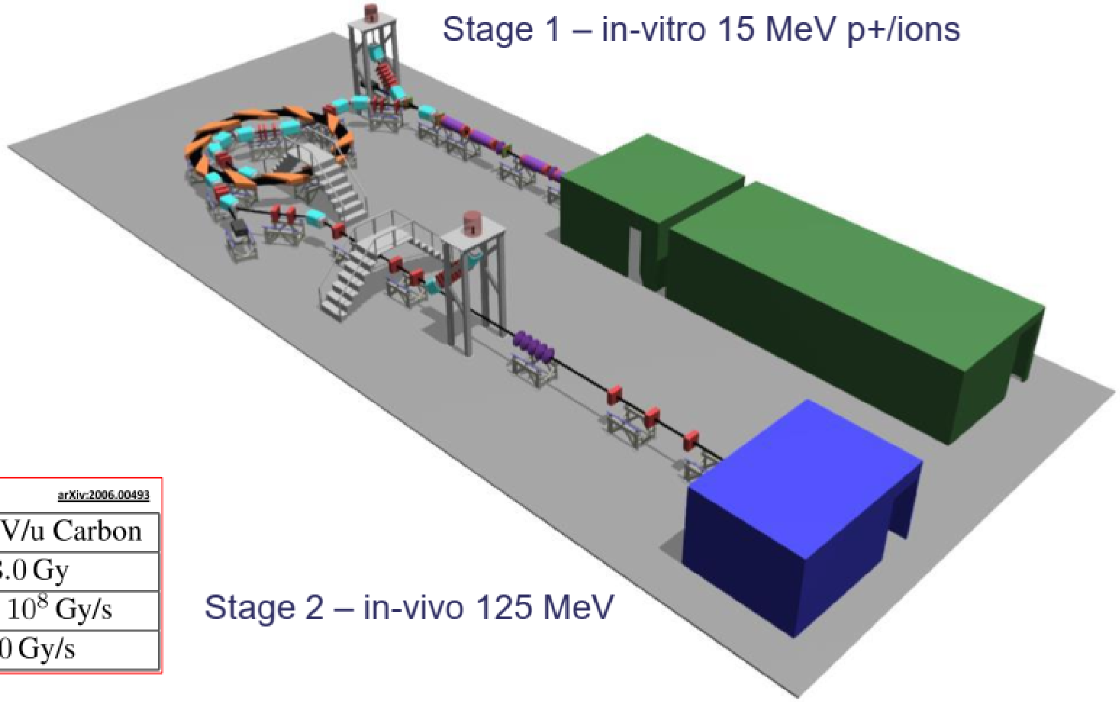

LhARA performance summary (arXiv:2006.00493)

	12 MeV Protons	15 MeV Protons	127 MeV Protons	33.4 MeV/u Carbon
Dose per pulse	7.1 Gy	12.8 Gy	15.6 Gy	73.0 Gy
Instantaneous dose rate	1.0×10^9 Gy/s	1.8×10^9 Gy/s	3.8×10^8 Gy/s	9.7×10^8 Gy/s
Average dose rate	71 Gy/s	128 Gy/s	156 Gy/s	730 Gy/s

- Stage 1: proton beams with energies in the range 12 MeV to 15 MeV to the Low-energy *in-vitro* End Station;
- Stage 2: proton beams of 127 MeV and ion beams of 33.4 MeV/nucleon to the High-energy *in-vitro* and *In-vivo* End Stations.

LhARA baseline design:
https://www.frontiersin.org/articles/10.3389/fphy.2020.567738/full

ITRF Research Need:
- Ion biology not yet well understood
- Likely benefits from heavier ions
- Clinical choice will require understanding of effects in tumour and normal tissue
- Ultimately might require individual patient research

Scintillator-based approach to dose mapping

Here we image the light arising from the proton beam, using a liquid scintillator contained within a 1000 mL volume.

This will be a cross-check on our ion-acoustic image and simulations.

The “Smart Phantom” with ports for optical cameras and external ultrasonic transducer arrays.

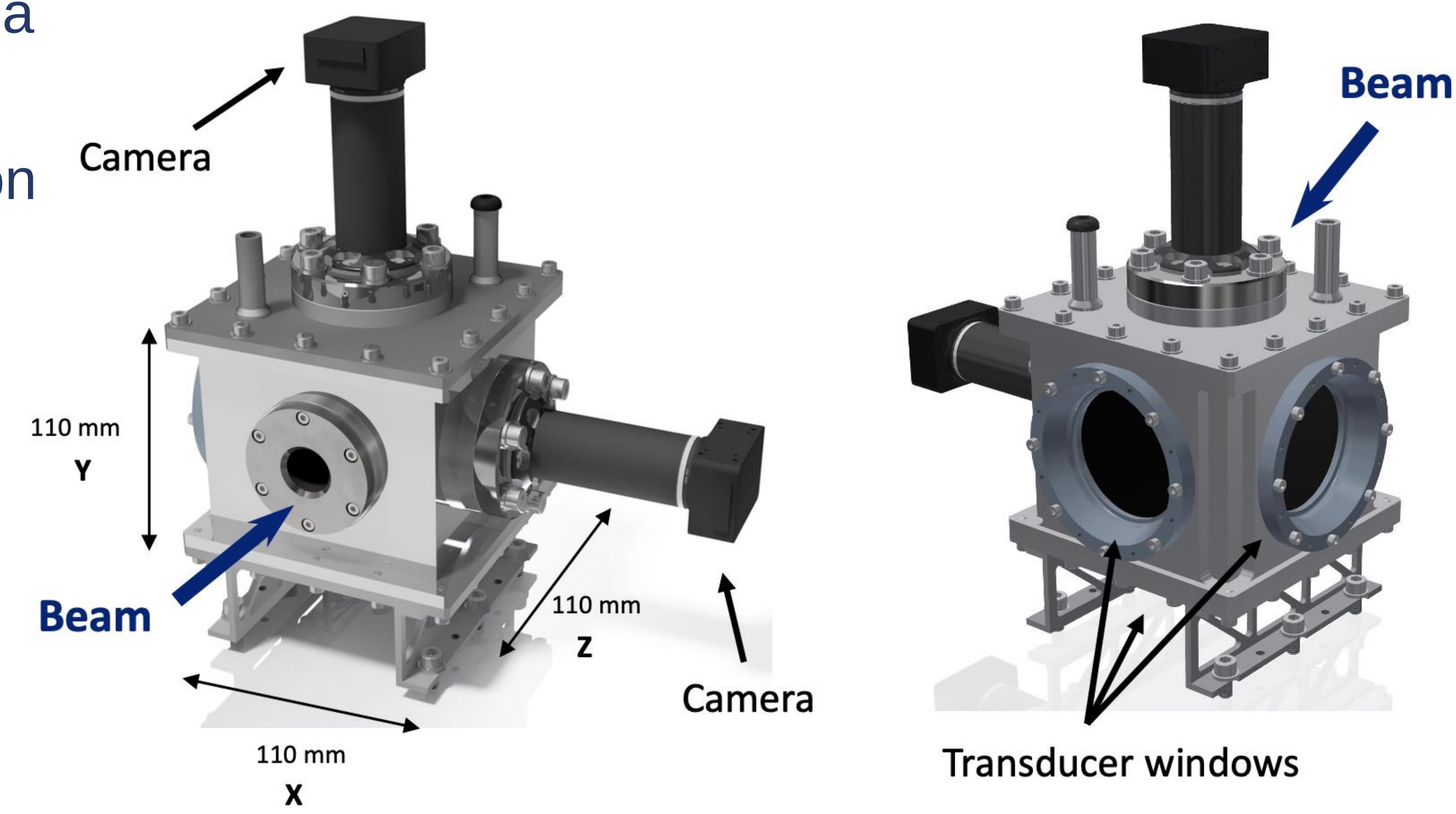

Simulating the scintillator-based approach

1. Scintillator is **UltimaGold™ XR** contained within the 100×100×100 mm^3 cube;
2. The scintillation yield is assumed to be 11200 photons per MeV deposited;
3. All scintillation light is modelled as a single wavelength of 427 nm;
4. Non-sequential rays are traced with "ray-splitting" enabled (i.e. Fresnel reflection and polarization is accounted for);
5. Imaging optics are a combination of two identical commercial achromatic lenses;
6. "Black" surfaces (Kapton™ and anodized aluminium) use **measured reflectance** (diffuse and specular);
7. The particle beam is modelled as an elliptical cylinder sub-divided into 0.5 mm thick slices. Each slice has a different intensity and rays are emitted isotropically in each slice;
8. Minimum relative ray intensity is 0.001, 1000 intersections per ray maximum;
9. Simulations use **Ansys ZEMAX OpticStudio 2023/2024 Pro** (PC is an i5 6/12 core @4.6 GHz peak with 32 Gbytes of 3200 MHz DDR4 memory).

Scintillator properties

Scintillator is UltimaGold™ XR. Peak emission wavelength: 427 nm

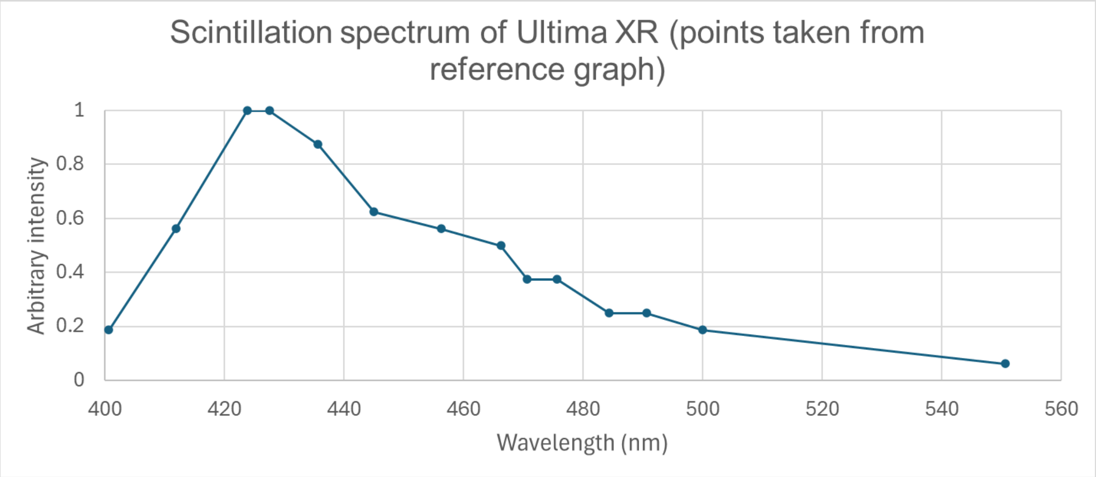

A commercial “cocktail” so some important details are not readily available.

Major component is Diisopropylnaphthalenes (DIPN), we model this in Geant4 as $C_{16}H_{20}$ with a density of 0.96 $g.cm^{-3}$ (real scintillator density).

				Wavelength (nm)								
Liquid											Temperature (C)	
	404.7	435.8	486.1	546.1	587.6	589.3	632.8	656.3	706.5			
Water	1.3432	1.3403	1.3372	1.3345	1.3335	1.3334	1.3321	1.3314	1.3301		20.0	
UltimaGold XR	1.5652	1.5553	1.5445	1.5362	1.5321	1.5320	1.5287	1.5272	1.5245		16.0	

Scintillation yield (photons/MeV) ~ 70% of anthracene. Anthracene yield is 16000 photons/MeV

Queen Mary
University of London
Science and Engineering

Applied Radiation and Isotopes **82** (2013) 382–388
Radiation Physics and Chemistry **84** (2013) 59–65

Deposited Energy from protons at 20 MeV nominal

The figure shows the average energy deposited per proton in the simulated DIPN. The simulation is for the LION beam at LMU Munich.

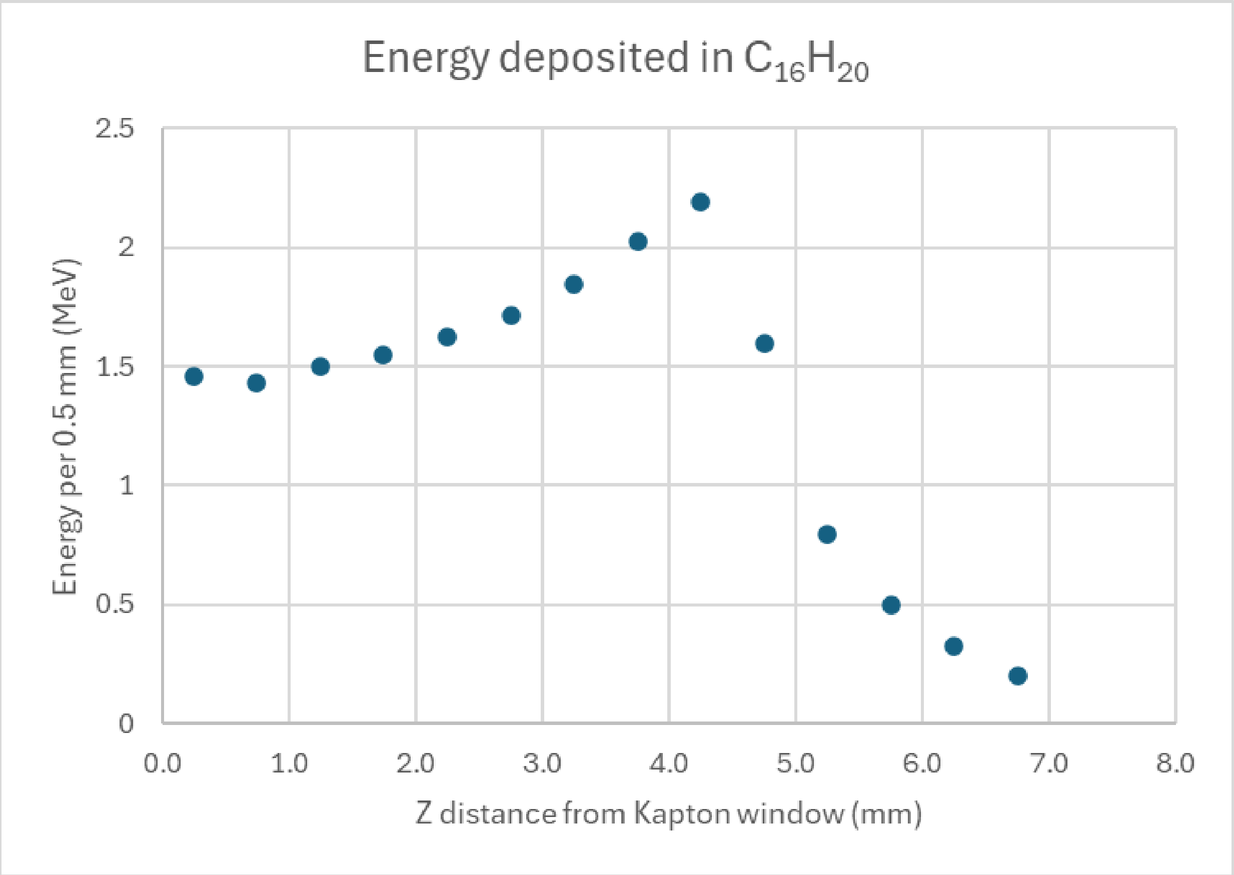

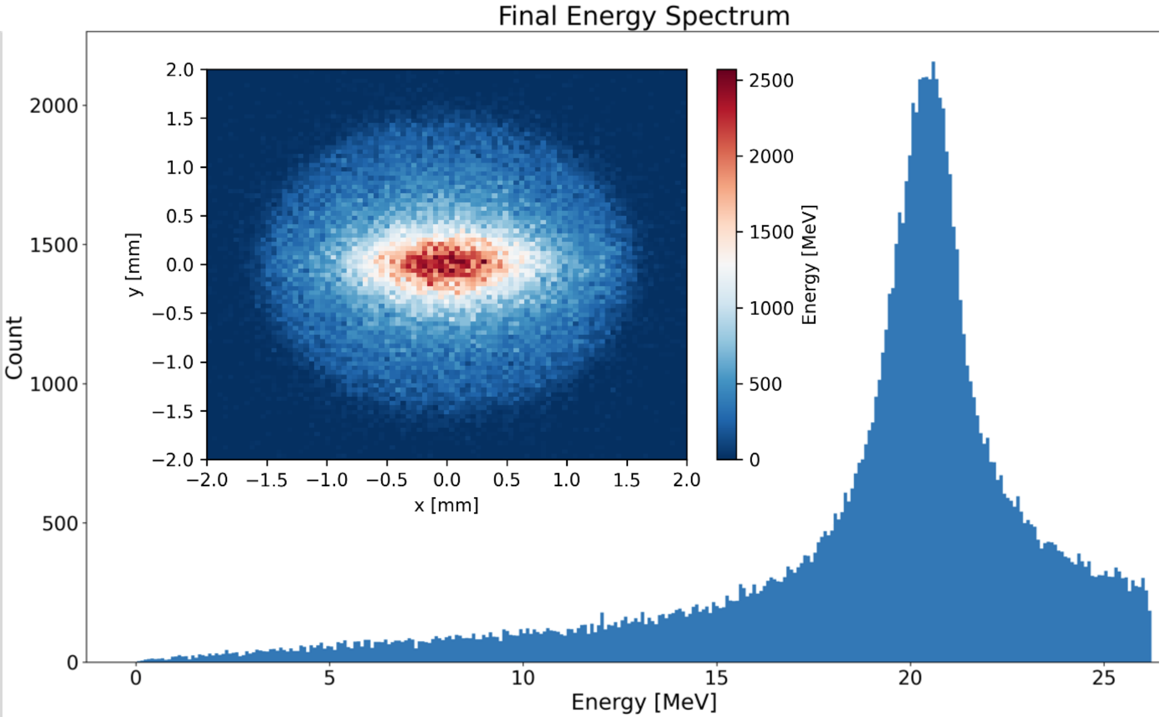

LION proton beam energy spectrum and (inset) beam profile

Modelled Smart Phantom

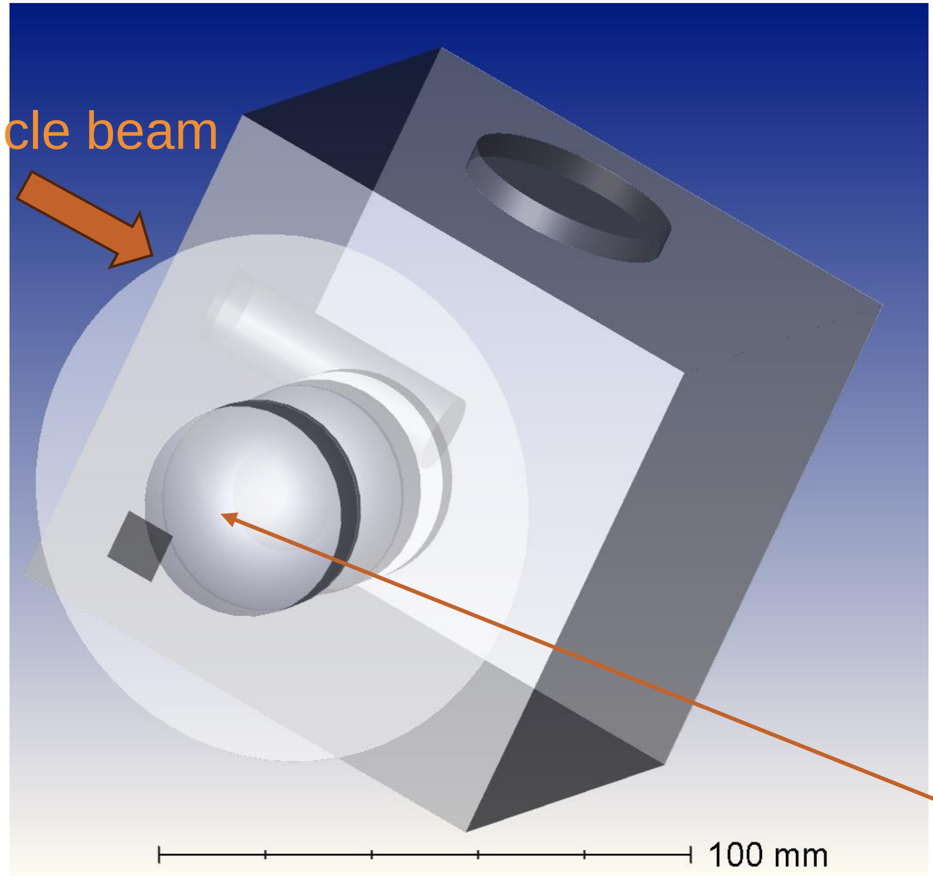

Optical window, lens, diaphragm and sensor (1 of 2 sets)

3D view of modelled volume. The second optical window is shown upper right.

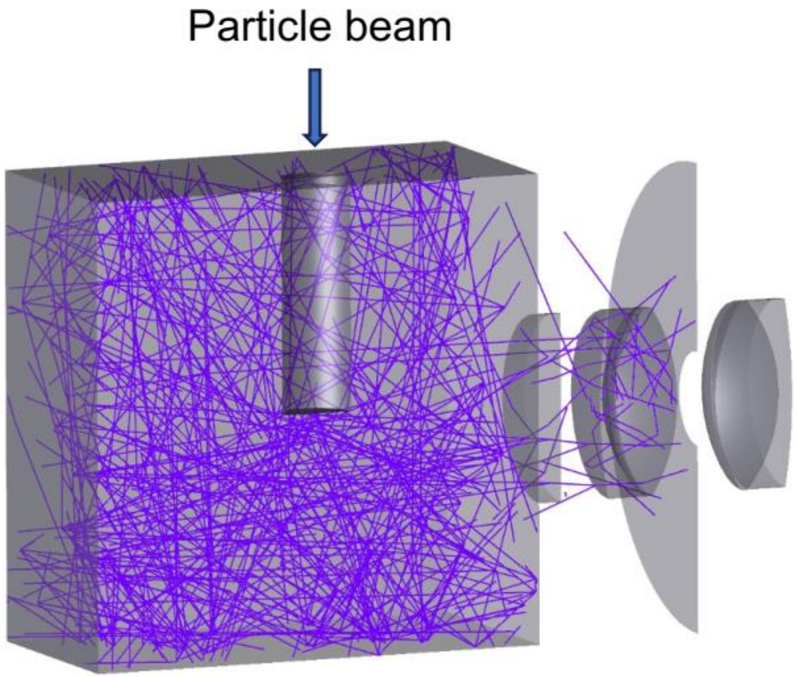

Zemax optical simulation of the phantom with liquid scintillator

Optical imaging system

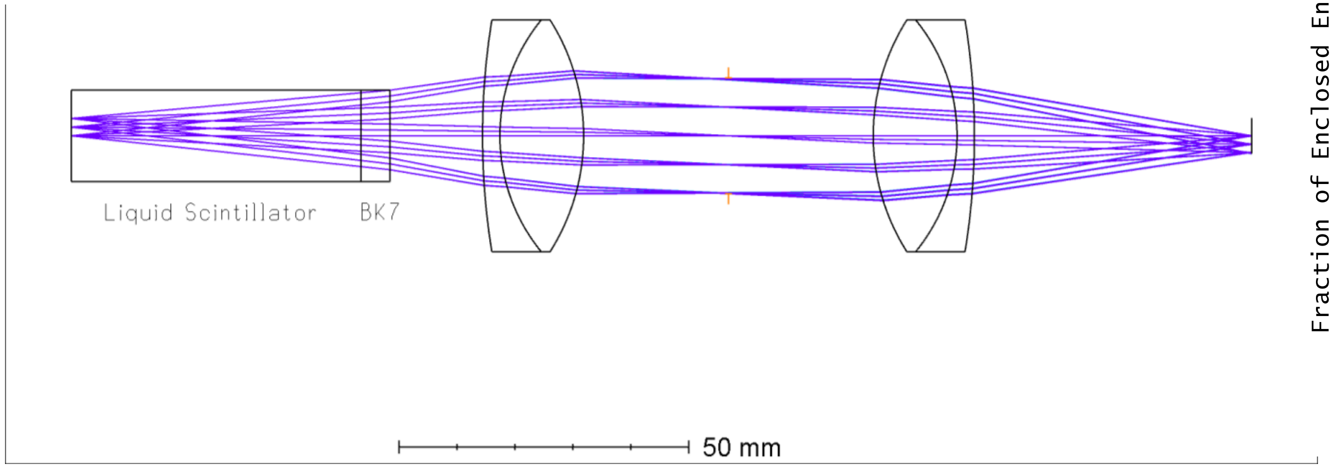

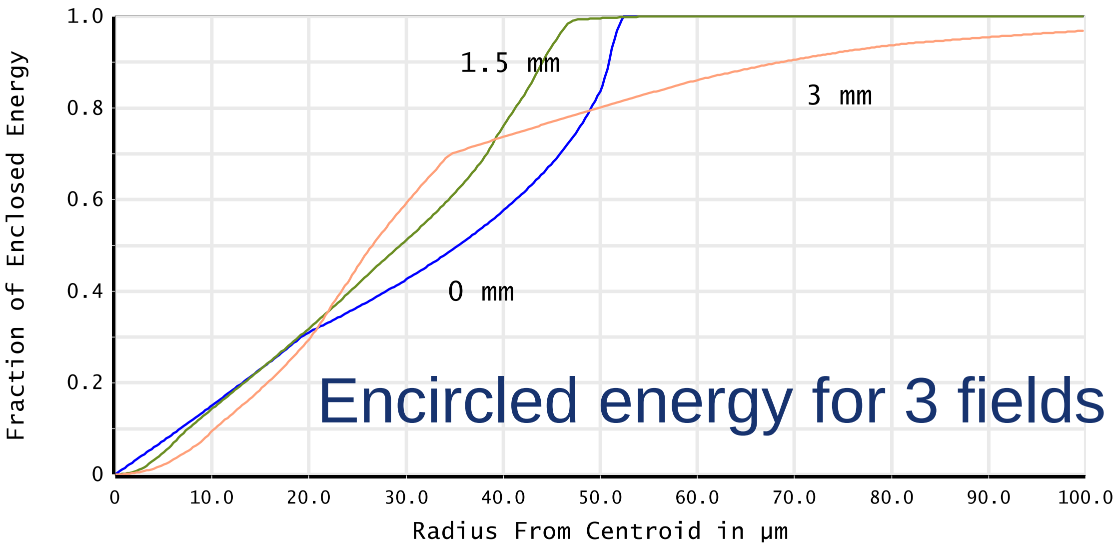

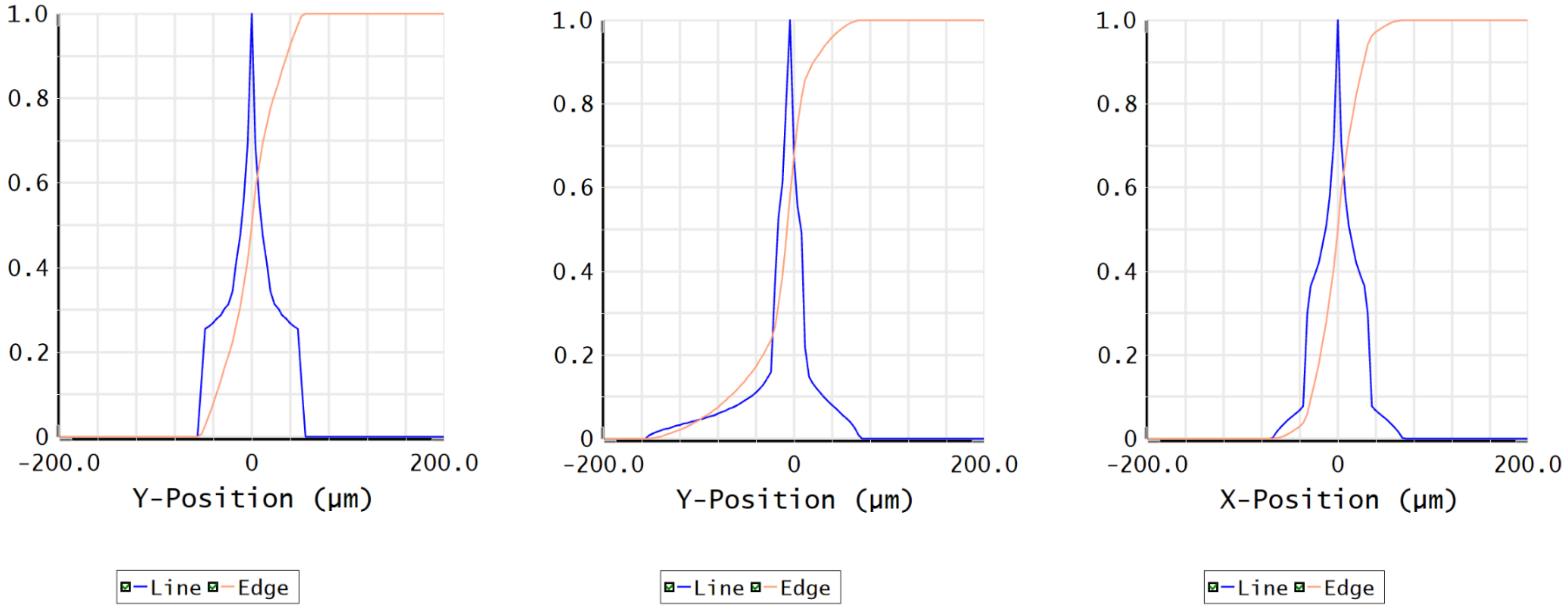

Geometric Line/Edge shown for on-axis and for the 3 mm off-axis fields.

Source model in ZEMAX Optic Studio

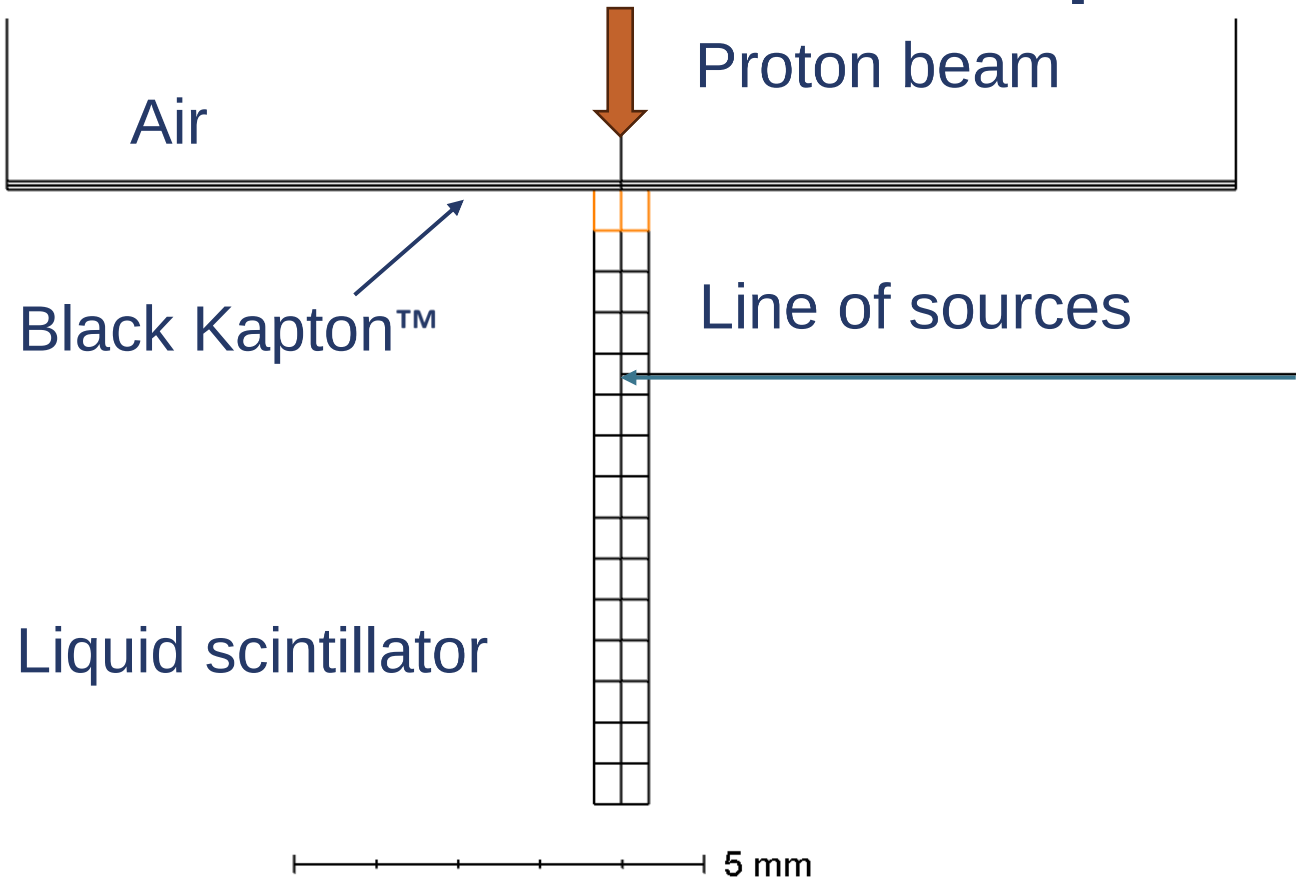

Source of scintillation photons is modelled as a line of elliptical elements each emitting isotropically. Intensity and # of photons are weighted by the simulated energy deposited in each 0.5 mm long elliptical cylinder.

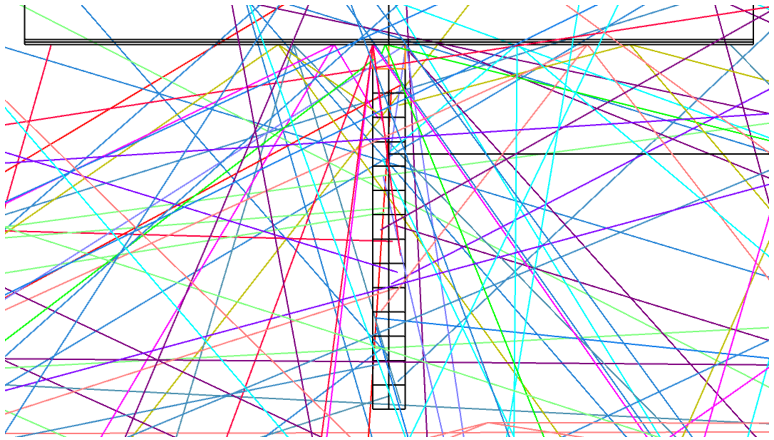

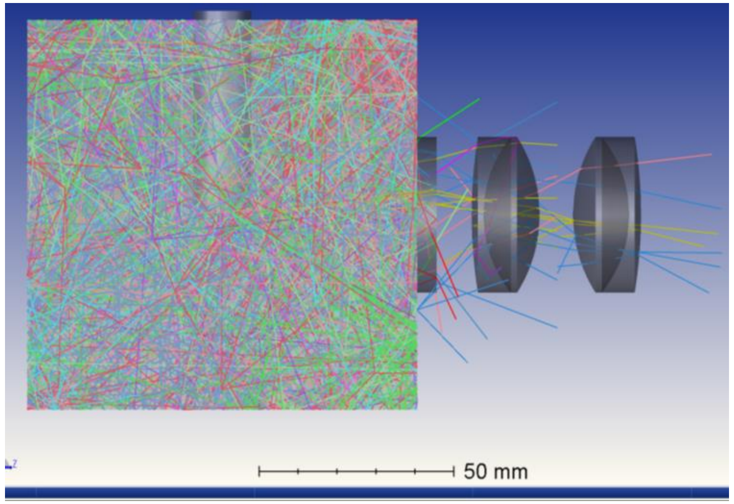

Only 2 primary rays per source are generated in this ray trace. Ray splitting and scattering are switched on.

Simulated image on camera

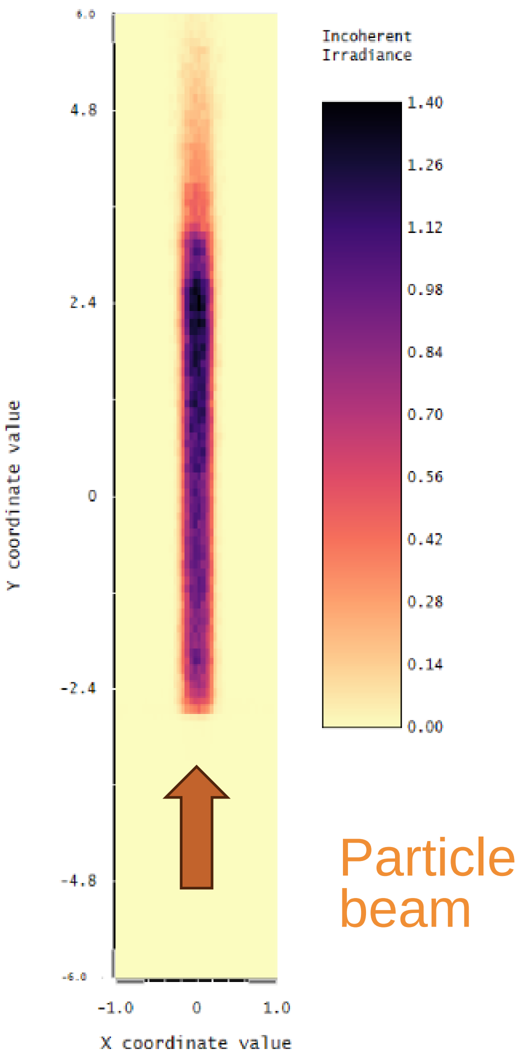

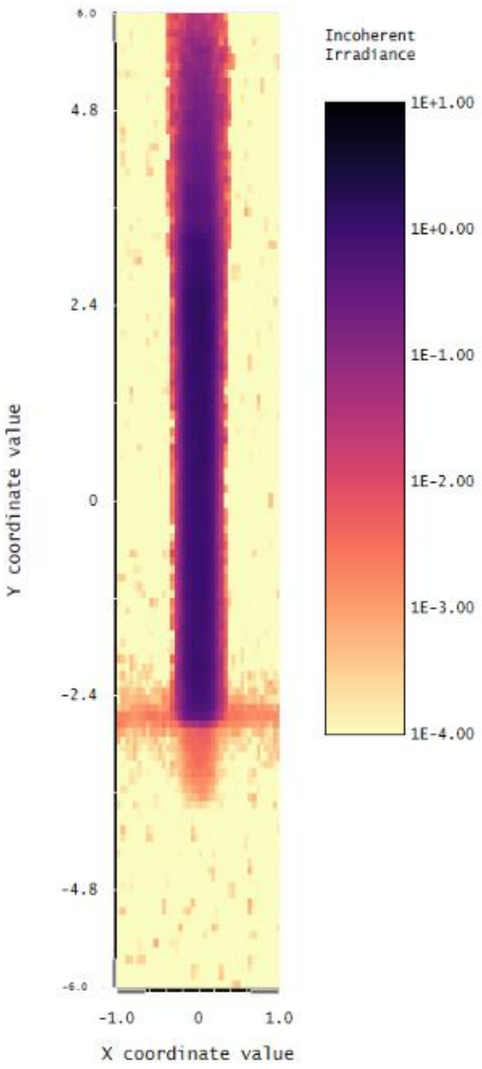

NOTES

50 µm × 100 µm pixels

21 million *primary* rays, have been generated to produce this image.

3 rays generated per Lambertian scatter event from “black” surfaces.

Optical collection efficiency is 0.3%

X, Y coordinates are in mm

Left figure is linear irradiance, right figure is logarithmic plot of the same data

Simulated image on camera

Cross-section along column centre of image on previous slide.

Both data sets, image and predicted energy deposit from the proton beam were normalised to total area and then to unity at the respective peaks.

NOTE

50 µm × 100 µm pixels

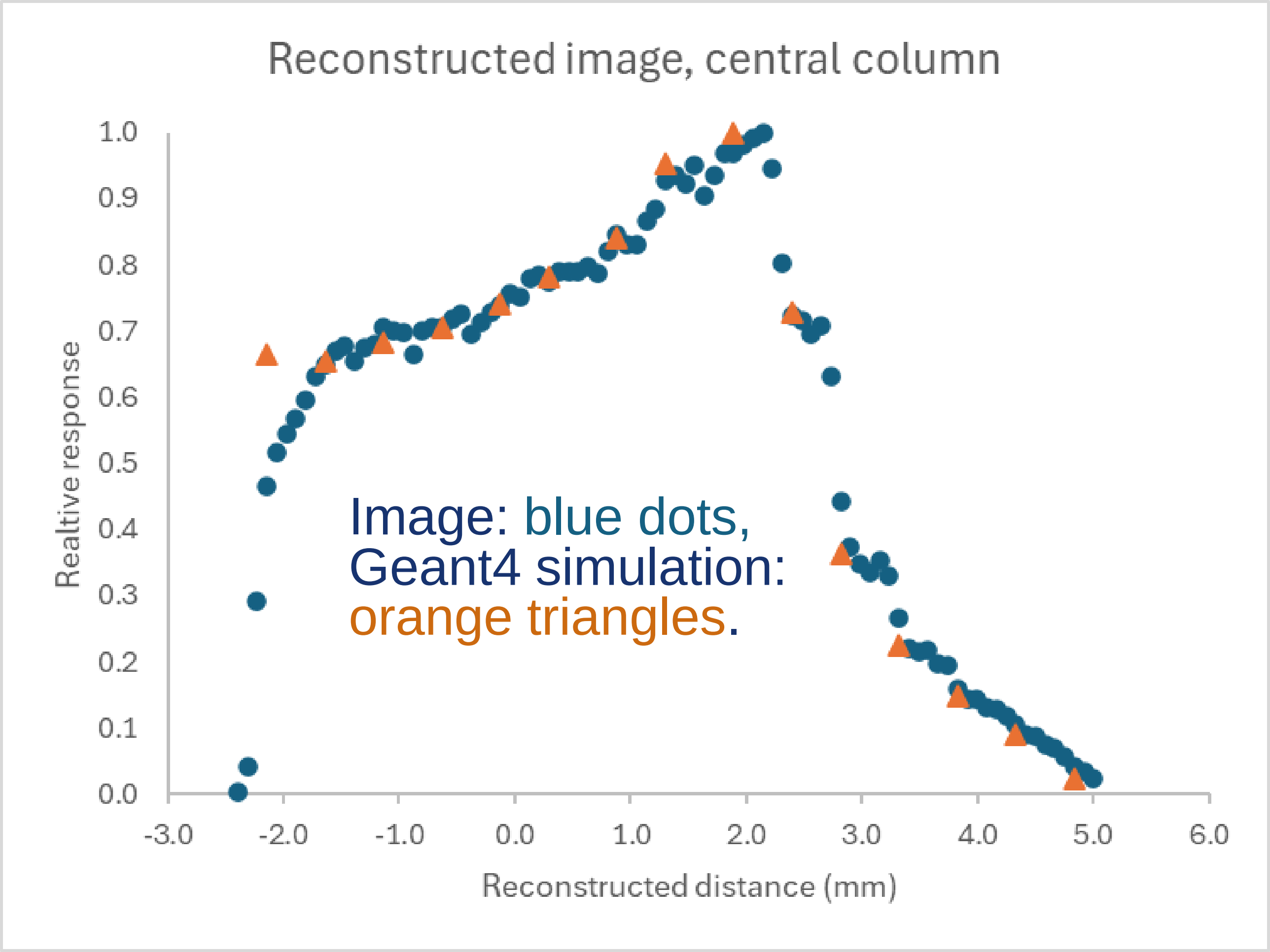

Actual image on camera from cyclotron proton beam

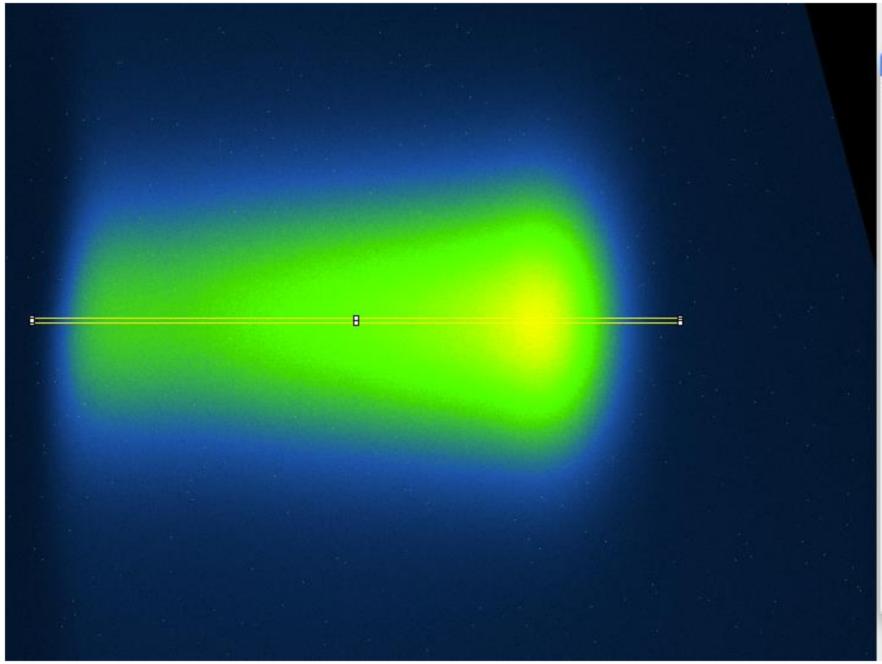

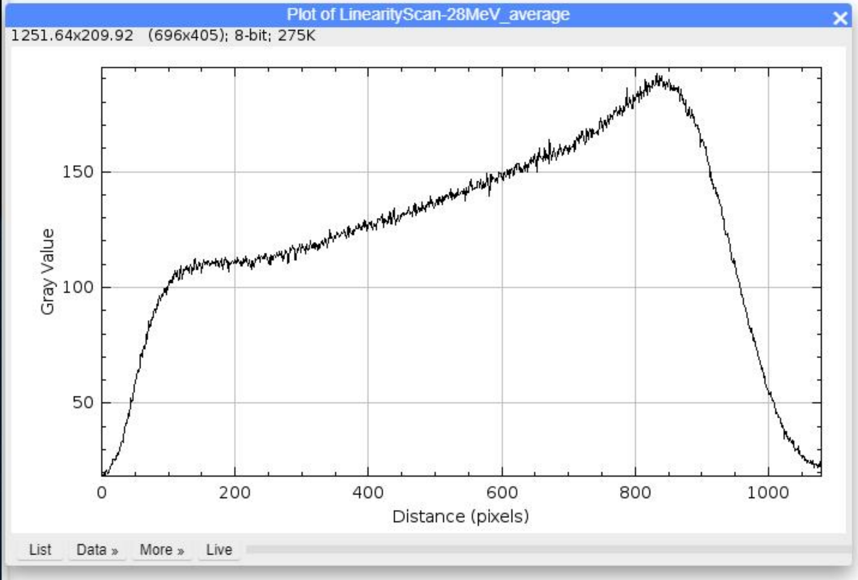

Camera

3.5 µm × 3.5 µm pixels

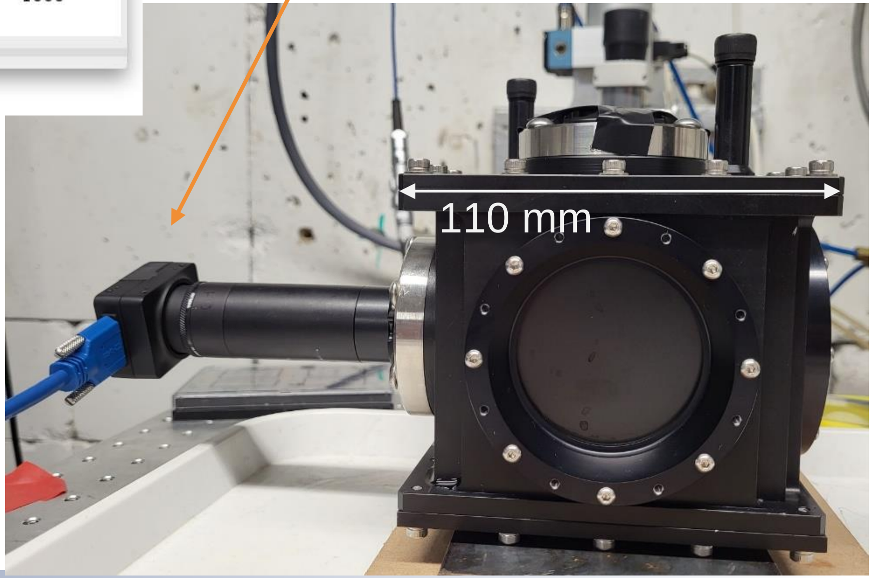

Very preliminary data from the UK Birmingham cyclotron (~20 MeV protons, 2 mm diameter beam collimator).

Average of 60 frames, dark frame subtracted. Profile plot is along the yellow rectangle.

Further work

Develop image correction procedures based on simulated synthetic sources;

Determine the sensitivity of the simulation to range of scintillation wavelengths (chromatic aberrations);

Include camera pixel readout noise;

Investigate the optical effect of including an acoustic sensor within the scintillator volume;

Fully analyse data from our recent, continuous accelerator test;

Test the system at a laser-driven accelerator and compare with ion-acoustic images.

The authors wish to acknowledge funding from the Science and Technology Facilities Council, UK